

## Resonant two-dimensional patterns in optical cavities with a rotated beam

Boris Y. Rubinstein and Len M. Pismen

*Department of Chemical Engineering and Minerva Center for Research in Nonlinear Phenomena,  
Technion-Israel Institute of Technology, Technion City, Haifa 32 000, Israel*

(Received 29 May 1997)

We describe selection and dynamics of transverse patterns in a nonlinear feedback cavity with a rotated beam. The symmetry of the patterns, described by composite modes, is determined by the image rotation angle within the loop. Complex quasicrystalline patterns sustained by resonant interactions arise under conditions when wave and Turing composite modes are excited simultaneously. It is shown that the excited patterns may be saturated even by the action of quadratic (three-wave) interactions only. Exact resonance involves three composite modes, and may exhibit periodic amplitude modulation on a slow time scale. Another possibility is a strained resonance leading to stabilization of the pattern in a wider parametric domain. Finally, wave-Turing resonance may be complemented by resonance among Turing triplets. [S1050-2947(97)09211-1]

PACS number(s): 42.65.Sf

### I. INTRODUCTION

Recent experiments based on nonlinear optical cavities with a rotated image beam [1–5] showed a variety of transverse patterns, including rolls, hexagons, rotating spirals, and various multipetal structures. Liquid crystals were chosen as a nonlinear medium in all these experiments. Observation of transverse patterns in real time was facilitated by the strong nonlinearity and slow response times of liquid crystals.

Akhmanov *et al.* [1] investigated both experimentally and numerically transverse patterns in a ring cavity containing a nonlinear element and a fiber bundle enabling one to rotate, shift, or dilate an optical image. In their simulations, they used a parabolic equation for the nonlinear phase shift in the nonlinear medium valid in the high absorption limit. This equation described various spatial transformations of the optical image (rotation, shift, dilation, and their combinations), as well as a time delay of the optical image in the feedback loop, but neglected diffraction. Linear stability analysis of this model, showing possible excitation of a variety of stationary (Turing) and wave modes with different symmetry, was carried out by Adachihiro and Faid [6]. The experiment [1] demonstrated excitation of rotating multipetal spiral structures, and their coexistence and hysteresis.

In the experiments reported by Pampaloni and co-workers [2–5], a liquid crystal light valve (LCLV) was used to close up the feedback loop. LCLV imitates a Kerr-like nonlinearity converting an amplitude deviation in the light beam into a phase modulation. In its turn, diffraction in a free propagation section of the optical cavity converts a phase shift into an amplitude modulation. The feedback loop is completed by a fiber bundle rotating the image by a certain angle. The experiment showed [2] that in the absence of rotation only hexagonal patterns are stable, while rotation by  $\pi$  leads to a stable roll structure. It was further shown [3] that periodic and quasiperiodic structures can be generated by rotating the image by an angle  $\Delta = 2\pi/N$  with an integer  $N > 4$ . Any of these structures corresponds to a family of  $N$  plane waves with the same wave number equispaced in Fourier space by the angle  $\Delta$ . Recent experiments [4,5] demonstrated simultaneous excitation of phase-locked families with different

wave numbers, leading to still more complicated quasicrystalline patterns.

Quasicrystalline patterns in experiments with a rotated optical beam may be viewed in a longer perspective of a quest for nonequilibrium patterns that have a complicated spatial structure but are well ordered in the Fourier space. It has been long expected that a variety of patterns of this kind may be constructed by considering interaction of competing wave modes near a symmetry-breaking bifurcation point [7]. It was predicted that such patterns may also exhibit complex dynamics of amplitude modulation on a slow time scale due to phase locking between noncollinear standing waves [8]. Another possible source of quasicrystalline patterns is a superposition of two resonant triplets of stationary (Turing) modes [9]. Conditions whereunder such patterns might be selected in reaction-diffusion or convective systems are apparently very rare, and are not easy to locate because of technical difficulties in evaluation of mode interaction coefficients. Quasicrystalline patterns of Turing type were, however, observed in experiments with parametric excitation of surface waves [10,11]. Selection of unforced quasicrystalline Turing patterns was discussed for model equations [12]; they were also shown to be one possible state of Marangoni convection in a layer with a deformable interface [13]. Optical systems may show more possibilities for formation of complex patterns. Selection of quasicrystalline patterns in a feedback cavity has been recently demonstrated analytically and numerically by Leduc *et al.* [14].

Optical systems with a rotated beam offer a most straightforward way to controlled spatiotemporal complexity, since here the symmetry of the pattern is imposed externally rather than being subject to a stringent selection process. Interaction among simultaneously excited modes of different wavelengths [4] is an additional way to greatly enhance complexity. In this case, pattern selection depends, however, on nonlinear interactions as in all “natural” nonequilibrium patterns.

Concerted selection of several modes is most likely when they are mutually enhanced as a result of resonant interactions [5]. Le Berre *et al.* [15] used this property to generate quasicrystalline Turing patterns with eightfold symmetry in a

special case when modes with the wave number ratio  $\sqrt{2}$  were excited simultaneously. Dynamical resonant patterns may occur when a Turing and wave mode are excited simultaneously. This is quite likely to occur in nonlinear optical cavities [16]. Logvin *et al.* [17] noticed a possibility of resonance between Turing and wave mode. This resonance has also been detected in Marangoni convection [18].

It is the aim of this paper to analyze dynamics of patterns generated through resonant interaction among families of bifurcating modes (or composite modes) of different type. After formulating the basic equations in Sec. II, we reiterate in Sec. III the linear analysis of the model discussed in Ref. [3], emphasizing simultaneous bifurcation of wave and Turing composite modes. Following the nonlinear analysis and derivation of amplitude equations (Sec. IV), we investigate in Sec. V long-time dynamics of composite patterns.

A specific feature of the system in question is a possibility of stabilization of a pattern by quadratic interactions only. Simple resonant patterns like a hexagonal one require for their stability a cubic (four-wave) interaction term to be included because quadratic (three-wave) terms alone cannot ensure amplitude saturation. Stabilization by quadratic interactions has been described before for restricting conditions of exact subharmonic resonance [18–20]. We shall see that composite patterns formed by two resonantly interacting families of modes may be stabilized by three-wave interactions in a wide parametric range, and show that the amplitudes of the constituent modes may undergo slow periodic modulation resulting in complicated spatiotemporal pattern dynamics. The exact resonance condition, verified by two wave modes and a single Turing mode, leads to complicated spatiotemporal patterns.

We shall also discuss (Sec. IV C) a possible *strained* resonance situation when only two composite modes (wave and Turing) survive. The wave mode is excited then with a wave number slightly different from the exact minimum of the neutral curve. Such a structure may be selected due to a strong mutual damping of modes directed at a small angle to one another. Strained resonance generally simplifies dynamics, and only stationary patterns are observed under these conditions. A special case considered in Sec. IV D is rotation by an angle  $\Delta = 2\pi/3N$  ( $N$  odd) when the wave-Turing resonance is complemented by the resonance among Turing trip-lets.

## II. BASIC EQUATIONS

The successive transformations of the complex envelope of the electric field  $E_i(\mathbf{r})$  of a light beam in a nonlinear optical cavity include three stages: (a) point transformation in the nonlinear medium, adding a phase  $n$  dependent on the transverse coordinate  $\mathbf{r}$ ; (b) diffraction in the empty part of the cavity, described by some linear operator  $\mathcal{D}$ , and (c) rotation of the image, described by the operator  $\mathcal{J}(\Delta)$ .

The first transformation takes place in a thin layer of a nonlinear Kerr-type medium, which is assumed to be uniform in the longitudinal direction. The field is transformed as

$$E_i(\mathbf{r}) \rightarrow R_1 E_i(\mathbf{r}) \exp(-i\chi(\mathbf{r}) + i\Omega), \quad (1)$$

where  $\chi$  is the normalized refractive index of the medium,  $\Omega$

is a constant phase shift, and  $R_1$  is the attenuation coefficient due to the absorption in the layer.

Propagation and diffraction of the beam in the free part of the cavity is described by the diffractive transform  $\mathcal{D}$  which is obtained in the paraxial approximation [21] as the resolvent of the parabolic equation

$$iE_z = \nabla^2 E. \quad (2)$$

Here the coordinate  $z$  in the direction of propagation is scaled by the length  $L$  of the diffractive path, and the transverse coordinates by the diffractive length  $\sqrt{L\lambda}$ , where  $\lambda$  is the wavelength;  $\nabla^2$  denotes the two-dimensional transverse Laplacian. Formally, one can write  $\mathcal{D}(z) = \exp(-iz\nabla^2)$ , so that  $\mathcal{D}(z) = \exp(izk^2)$  when it operates upon a pure mode with a transverse wave number  $k$ .

Before closing the loop, the image is rotated by a certain angle  $\Delta$ . The rotation is described by the operator

$$\mathcal{J}(\Delta): \mathcal{J}(\Delta)\{r, \phi\} = \{r, \phi + \Delta\}. \quad (3)$$

The resulting output field  $E_o$  can be written as

$$E_o(\mathbf{r}) = \mathcal{J}(\Delta)R\mathcal{D}(1)E_i(\mathbf{r})\exp[-i\chi(\mathbf{r}) + i\Omega], \quad (4)$$

where the attenuation coefficient  $R$  lumps all losses during a single round-trip.

The model of material dynamics can be written, assuming a Kerr-type nonlinearity, in the dimensionless form [22]

$$\dot{\chi} = \delta^2 \nabla^2 \chi - \chi - \kappa_1 |E_o(\chi(\mathbf{r}))|^2. \quad (5)$$

The material response time is taken as the time scale;  $\delta$  is the ratio of the photocarrier diffusion length to the diffraction length. Although typically  $\delta \ll 1$ , the thin sample approximation can be retained, provided the diffusional length far exceeds  $\lambda$ , so that longitudinal wavelength scale grating is washed out by diffusion. Then Eq. (5) retains only the transverse Laplacian  $\nabla^2$ . Dynamics of the refractive index modulation  $\chi$  depends on the strength of the nonlinearity  $\kappa_1$ , which is positive for a defocusing medium.

We shall assume that the material response time is much larger than the round-trip time in the cavity. Under these conditions, the electric field envelope is quasistationary, being slaved to the material variable. Combining the cavity transform Eq. (4) with the appropriate feedback conditions then allows expression of  $E(\mathbf{r})$  as a nonlinear functional of the material field  $\chi(\mathbf{r})$ . Now Eq. (5) is rewritten as

$$\dot{\chi} = \delta^2 \nabla^2 \chi - \chi - \kappa \mathcal{J}(\Delta)I \exp(-i\nabla^2) \exp(-i\chi)^2, \quad (6)$$

where  $I$  denotes the input beam intensity and  $\kappa = \kappa_1 R^2$ .

Equation (6) always has a stationary homogeneous solution  $\chi_0 = -\kappa I$  which, however, may lose stability when the input intensity exceeds a certain critical level. The critical intensity, as well as the preferred transverse wavelength of the emerging pattern, is determined by the linear stability analysis of the homogeneous solution.

## III. LINEAR ANALYSIS

The standard procedure of linear analysis involves testing stability to arbitrary infinitesimal perturbations, usually plane

waves. The rotation of the optical field mixes different Fourier modes, and thereby limits the choice of basis functions. If the rotation angle is commensurate with  $2\pi$ , so that  $\Delta = 2\pi n/N$  (where  $n$  and  $N$  are integers that do not have common factors), one can use a rotationally invariant combination of  $N$  plane waves  $\exp(i\mathbf{q}_j \cdot \mathbf{r})$ , where  $|\mathbf{q}_j| = q = \text{idem}$ , and  $\arg(\mathbf{q}_j) = \Delta j, j = 0, 1, \dots, N-1$ , and their complex conjugates. This combination corresponds to a regular pattern at  $N \leq 4$  or  $N = 6$ , and to a quasicrystalline planform at other  $N$ . Since the emerging pattern must be stationary at the round-trip time scale, the amplitudes of all constituent modes should have identical moduli, but their phases may be different.

We shall reiterate here in more detail the linear analysis outlined in Ref. [3] for the case of a commensurate rotation angle  $\Delta = 2\pi/N$  with integer  $N$ . Proceeding in a standard way, we set  $\chi = \chi_0 + \epsilon \chi_1(\mathbf{r}, t)$ , where  $\epsilon \ll 1$ , and linearize Eq. (6) presenting the linear term  $\chi_1$  as the sum of  $N$  bifurcating modes with the wave vectors  $\mathbf{q}_i$  ( $i = 1, 2, \dots, N$ ) equally spaced by the angle  $\Delta$ , and their conjugates:

$$\chi_1 = \sum_{j=1}^N a_j \exp(i\mathbf{q}_j \cdot \mathbf{r} + \lambda t) + \text{c.c.} \quad (7)$$

The linear eigenvalue problem then reads

$$\mathcal{L}\chi_1 = [\lambda + 1 + \delta^2 q^2 + 2\kappa I \sin(q^2) \mathcal{J}(\Delta)] \chi_1 = 0. \quad (8)$$

Because the action of the rotation operator has the form  $\mathcal{J}(\Delta)\mathbf{q}_i = \mathbf{q}_{i+1}$ , the term  $\mathcal{J}(\Delta)\chi_1$  is expressed as

$$\mathcal{J}(\Delta)\chi_1 = \sum_{j=1}^N a_j \exp(i\mathbf{q}_{j+1} \cdot \mathbf{r} + \lambda t) + \text{c.c.}, \quad (9)$$

where the indices are cyclic modulo  $N$ . The amplitude vector  $\mathbf{a}$  comprised of the amplitudes  $a_j$  satisfies the eigenvalue problem  $\mathbf{M}\mathbf{a} = \lambda\mathbf{a}$  with a circulant matrix  $\mathbf{M}$ , such that  $\mathbf{M}_{i,i} = -(1 + \delta^2 q^2)$  and  $\mathbf{M}_{i,i-1} = -2\kappa I \sin q^2$ ; all other elements of  $\mathbf{M}$  are zeroes. The set of eigenvalues of the matrix  $\mathbf{M}$  is

$$\lambda_i = -(1 + \delta^2 q^2 + 2\kappa I r_j^{N-1} \sin q^2). \quad (10)$$

The components  $\mathbf{U}_{j,k}$  of the corresponding eigenvectors  $\mathbf{U}_j$  are

$$\mathbf{U}_{j,k} = r_j^{k-1} \equiv e^{2\pi i j k / N}, \quad j = 1, \dots, N \quad (11)$$

where  $r_j$  denotes the  $j$ th root of unity of  $N$ th degree.

The basic state  $\chi_0$  loses stability at  $\text{Re}\lambda_j = 0$ , which determines the location of the neutral curve:

$$I = -\frac{1 + \delta^2 q^2}{2\kappa \sin q^2 \cos(\Delta j)}. \quad (12)$$

The positive branches of this curve give the critical value of the bifurcation parameter  $I_{cr}$  corresponding to excitation of a planform with the wave number  $q$ . The selected type of planform and the wave number correspond to the absolute minimum of  $I(q)$ .

The cases of even and odd values of  $N$  should be considered separately.

### A. Even $N$

The lowest positive value of the bifurcation parameter  $I$  is reached at  $j = N/2$  and is

$$I = \frac{1 + \delta^2 q^2}{2\kappa \sin q^2}. \quad (13)$$

The corresponding eigenvector (11) with  $j = N/2$  has real components  $\mathbf{U}_{N/2,k} = (-1)^{k-1}$ , and the excited planform is described by

$$\chi_1 = a \sum_{k=1}^N (-1)^{k-1} \exp(i\mathbf{q}_k \cdot \mathbf{r}) + \text{c.c.} \quad (14)$$

Here again two cases arise. The first one corresponds to  $N = 4K$  with integer  $K$ , giving

$$\chi_1 = A \sum_{k=1}^{N/2} (-1)^{k-1} \cos(\mathbf{q}_k \cdot \mathbf{r}). \quad (15)$$

Another possibility is  $N = 2(2K - 1)$  with

$$\chi_1 = A \sum_{k=1}^{N/2} \sin(\mathbf{q}_k \cdot \mathbf{r}). \quad (16)$$

In the last two formulas, the amplitude  $A$  is real.

We observe that for even  $N$  the bifurcating planform is a combination of  $N$  Turing modes. All these modes are excited simultaneously, so we consider a single *composite* Turing mode with the amplitude  $a$ .

### B. Odd $N$

The case of odd  $N$  is most interesting because it provides a possibility of a resonance among composite modes bifurcating at different wavelengths. The lowest minima of positive branches may have close heights. Such minima are reached at  $j = (N+1)/2$  and  $N$ , respectively.

For the  $j = N$ , the eigenvalue is real:

$$\lambda_N = -(1 + \delta^2 q^2) - 2\kappa I \sin q^2. \quad (17)$$

The neutral curve is given by

$$I = -\frac{1 + \delta^2 q^2}{2\kappa \sin q^2}. \quad (18)$$

The amplitudes of the elementary modes are equal to one another:

$$\mathbf{U}_{N,k} = 1, \quad a_j = a. \quad (19)$$

As the result a composite Turing mode is excited:

$$\chi_1 = a \sum_{k=1}^N \exp(i\mathbf{q}_k \cdot \mathbf{r}) + \text{c.c.} \quad (20)$$

In the case  $j = (N+1)/2$ , the eigenvalue is complex:

$$\lambda_{(N+1)/2} = -(1 + \delta^2 q^2) + 2\kappa I \sin q^2 \exp(i\Delta/2). \quad (21)$$

The critical value of the bifurcation parameter  $I$  is

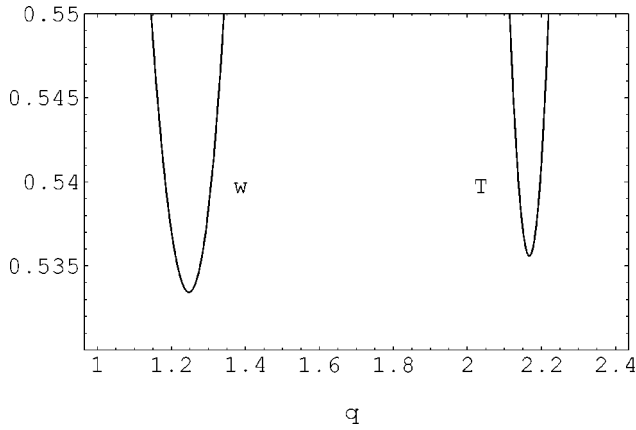


FIG. 1. First two positive branches of the neutral curve for  $N=11$ , corresponding to a composite wave mode ( $w$ ), and a composite Turing mode ( $T$ ).

$$I = \frac{1 + \delta^2 q^2}{2\kappa \cos(\Delta/2) \sin q^2}. \quad (22)$$

The emerging structure can be characterized as a composite wave mode with a nonzero frequency

$$\omega = (1 + \delta^2 q^2) \tan(\Delta/2). \quad (23)$$

The eigenvector (11) has complex-valued components:

$$\mathbf{U}_{(N+1)/2,k} = (-e^{i\Delta/2})^{k-1}. \quad (24)$$

The last result implies the relation between the amplitudes of the adjacent modes

$$a_{j-1} = -a_j e^{-i\Delta/2}. \quad (25)$$

Finally, the excited composite wave mode is

$$\chi_1 = a e^{i\omega t} \sum_{k=1}^N (-1)^{k-1} e^{i(k-1)\Delta/2} \exp(i\mathbf{q}_k \cdot \mathbf{r}) + \text{c.c.} \quad (26)$$

### C. Degenerate bifurcations

In the diffractive limit,  $\delta \ll 2\pi/q$ , all branches have minima at  $q^2 = (2m+1)\pi/2$  with integer  $m$ . Only first branches which have the lowest minima are relevant for the pattern selection. The wave mode has the lowest minimum at  $q = \sqrt{\pi/2}$ , while the first positive minimum of the Turing mode is located at  $q = \sqrt{3}\pi/2$ .

It can be shown that for small odd  $N$  the composite Turing mode is most dangerous, while for large  $N$  the composite wave mode has the lowest threshold. It is easy to determine the critical value of  $N$  when both modes can be excited simultaneously. This value is given by

$$N_{\text{cr}} = (1/\pi) \arccos \frac{1 + 2/(\pi\delta^2)}{3 + 2/(\pi\delta^2)}. \quad (27)$$

The calculations using the values of the parameters reported in [3] give the best fit integer value  $N=11$ . The first two positive branches of the neutral curve  $I(q)$  for the composite wave and Turing modes each comprised of 11 plane wave

modes are shown in Fig. 1. Their minima are close one to the other, and both may be excited simultaneously.

## IV. WEAKLY NONLINEAR ANALYSIS

### A. Multiscale expansion

Following the standard method of multiscale expansion, we introduce a hierarchy of time scales:

$$\partial/\partial t = \partial/\partial t_0 + \epsilon \partial/\partial t_1 + \epsilon^2 \partial/\partial t_2 + \dots, \quad (28)$$

and expand in Taylor series the phase variable and the bifurcation parameter:

$$\chi = \chi_0 + \epsilon \chi_1 + \epsilon^2 \chi_2 + \dots, \quad I = I_0 + \epsilon I_1 + \epsilon^2 I_2 + \dots. \quad (29)$$

In order to exclude the dependence of the basic solution  $\chi_0$  on the bifurcation parameter, we shift the variable  $\chi \rightarrow \chi - \chi_0$ ; then Eq. (6) becomes

$$\dot{\chi} = \delta^2 \nabla^2 \chi - \chi - \kappa \mathcal{J}(\Delta) I |\exp(-i\nabla^2) \exp(-i\chi)|^2 + \kappa I, \quad (30)$$

with the trivial basic solution  $\chi=0$ .

Using the above expansions in Eq. (30) we recover in the first order in  $\epsilon$  the linear eigenvalue problem (8). In the next order, we arrive at the following inhomogeneous linear problem:

$$\begin{aligned} \mathcal{L}\chi_2 = & -\partial\chi_1/\partial t_1 - 2\kappa I_0 \sin^2(\nabla^2/2) \mathcal{J}(\Delta) \chi_1^2 \\ & + 2\kappa I_1 \sin(\nabla^2) \mathcal{J}(\Delta) \chi_1, \end{aligned} \quad (31)$$

where  $\mathcal{L}$  is defined in Eq. (8). Amplitude equations are obtained as solvability conditions of Eq. (31), i.e., conditions of orthogonality of the inhomogeneity to all eigenfunctions of the adjoint linear problem. A nontrivial solvability condition is obtained when the quadratic term (a product of two eigenfunctions, say,  $\psi_1$  and  $\psi_2$ ) is *in resonance* with another eigenmode, say,  $\psi_0$ . This requires that the frequencies and wave numbers of the three modes involved satisfy the conditions

$$\mathbf{k}_1 + \mathbf{k}_2 = \mathbf{k}_0, \quad \omega_1 + \omega_2 = \omega_0. \quad (32)$$

A resonance triplet may involve therefore either three Turing modes or two wave modes from the same family (i.e., with identical frequencies) and one Turing mode.

### B. Exact resonance

A possible resonant structure that may be excited at odd  $N$  consists of two wave modes with a wave number  $q$  and one Turing mode with the wave number  $Q = \sqrt{3}q$ .  $N$  such modes must be present to satisfy the imposed rotational symmetry. The pattern in the Fourier space is built of  $N$  identical isosceles triangles with acute angles equal to  $\pi/6$  (and their conjugates produced by rotating the original triangles by  $\pi$ ). The triangles are spaced by the angle  $\Delta = 2\pi/N$ . Altogether, this resonant planform is built of  $6N$  plane wave modes:

$$\chi_1 = \sum_{j=1}^N \{a_j e^{i\mathbf{Q}_j \cdot \mathbf{r}} + e^{i\omega t} (b_j e^{i\mathbf{q}_j \cdot \mathbf{r}} + c_j e^{i\mathbf{k}_j \cdot \mathbf{r}})\} + \text{c.c.}, \quad (33)$$

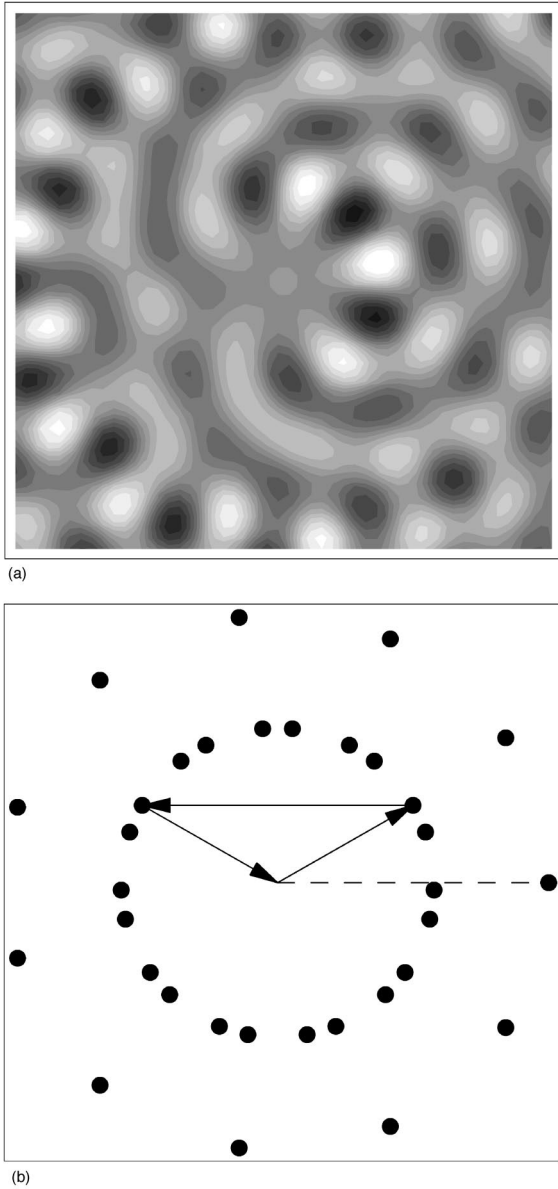


FIG. 2. The planform (33) with  $N=11$ . (a) A snapshot of a real space (near field) image. The values or the amplitudes correspond to the periodic solution at  $\mu=-1/20$  (Fig. 4) taken at  $t=178$ . (b) The structure in the Fourier space (far field image). The inner circle corresponds to wave modes, and the outer circle to Turing modes. Complex conjugate modes are omitted. One of the resonant isosceles triangles is shown, and the participating Turing mode is indicated by the dashed line.

where the complex conjugate is added for odd  $N$ ,  $q_j=k=Q/\sqrt{3}$ , and the following relations are satisfied:

$$\begin{aligned} \mathbf{q}_j - \mathbf{k}_j &= \mathbf{Q}_j, \quad a_{j+1} = a_j, \\ b_{j+1} &= -e^{i\Delta/2} b_j, \quad c_{j+1} = -e^{i\Delta/2} c_j. \end{aligned} \quad (34)$$

The first of these is the resonance condition (32). The three reciprocity relations imposed by the rotational symmetry follow from Eqs. (19) and (24).

A snapshot of the pattern defined by Eq. (33) and the corresponding structure in the Fourier space are shown in Fig. 2. The planform has a complicated nonstationary quasi-

crystalline structure. Since the plane waves comprising the pattern are out of phase by  $\Delta/2$ , the pattern exhibits rotational motion at each location.

In order to derive dynamic equations for the amplitudes  $a_j$ ,  $b_j$ , and  $c_j$ , one has to substitute Eq. (33) in the right hand side of Eq. (31), and then to project it on the adjoint eigenvector  $\mathbf{U}^\dagger$  satisfying  $\mathcal{L}^\dagger \mathbf{U}^\dagger = \mathbf{0}$ , where  $\mathcal{L}^\dagger = \mathcal{L}^*$  is the operator adjoint to  $\mathcal{L}$ .

Using the relations (34) we arrive after some algebra at the following system of amplitude equations:

$$\begin{aligned} \dot{a}_j &= -2\kappa I_0 \sin^2(Q^2/2) b_j c_j^* - 2\kappa I_{1s} \sin^2 Q^2 a_j, \\ \dot{b}_j &= e^{-i\Delta/2} [2\kappa I_0 \sin^2(q^2/2) a_j c_j + 2\kappa I_{1w} \sin q^2 b_j], \\ \dot{c}_j &= e^{-i\Delta/2} [2\kappa I_0 \sin^2(q^2/2) a_j^* b_j + 2\kappa I_{1w} \sin q^2 c_j]. \end{aligned} \quad (35)$$

Here  $I_{1s}$  and  $I_{1w}$  denote small deviations from the critical value  $I_0$  for the Turing (stationary) and wave composite modes, respectively. These deviations may have different signs due to different values of the corresponding minima of the neutral curve. Further on, we choose them to be of the opposite sign. This means that one of the composite modes is subcritical and the other one is supercritical. This case is most interesting, as it allows us to prevent both decay to the trivial state and runaway to large amplitudes through the action of quadratic interactions.

Recalling that  $q^2 = \pi/2$  and  $Q^2 = 3\pi/2$  we rewrite the above system as

$$\begin{aligned} \dot{a}_j &= \mu_s a_j - \nu b_j c_j^*, \\ \dot{b}_j &= (\mu_w b_j + \nu a_j c_j) e^{-i\Delta/2}, \\ \dot{c}_j &= (\mu_w c_j + \nu a_j^* b_j) e^{-i\Delta/2}, \end{aligned} \quad (36)$$

where  $\nu = \kappa I_0$ ,  $\mu_s = 2\kappa I_{1s}$ , and  $\mu_w = 2\kappa I_{1w}$ . A similar dynamical system has been obtained in the context of Marangoni convection [18], although there the setting was one dimensional, and therefore the resonance occurred only under conditions when the wave number of the Turing mode was exactly twice that of the wave mode. This restriction is lifted in two dimensions, as the resonance condition (32) can be satisfied in a wide range of wave number ratios by choosing an appropriate angle between the wave vectors.

### C. Strained resonance

One can also envisage a structure based on a single composite wave mode and a single composite Turing mode. It is clear that, while in this structure all resonant triangles remain isosceles, the acute angles have slightly different values, and the wavelengths must be different from the exact minima of the neutral curve. We call it therefore a *strained* resonance.

Excitation of a strained planform is likely for the following reason. The smallest angle between two wave modes involved in the exact resonant planform corresponds to a mismatch between  $m\pi/N$  and  $n\pi/6$ , where  $m, n$  are integers, and comes for  $N=11$  to a mere  $\pi/66$ , i.e., less than  $3^\circ$ . Modes at very small acute angles are expected to be strongly mutually damping by cubic interactions. Generally, we expect that cubic interaction coefficients smoothly depend on

the angle between the modes, and therefore interactions at a small angle do not differ very much from interactions at zero angle. The self-interaction coefficient is, for combinatorial reasons, exactly one-half the interaction coefficient of two modes at zero angle, and therefore waves at small angles would tend to “merge.” Although cubic interactions are weaker than quadratic ones at small amplitudes, and we do not consider them here explicitly, we may expect that the system might choose to reduce the number of modes and adjust to the resonance by straining the wavelength slightly off the optimal value.

We assume that the vectors of the composite wave mode  $\mathbf{q}_j$  and  $\mathbf{q}_{j+n}$  are in resonance with the vector  $\mathbf{Q}_j$  of the Turing composite mode:  $\mathbf{Q}_j + \mathbf{q}_{j+n} = \mathbf{q}_j$ . If the vector  $\mathbf{q}_j$  is at an angle  $\alpha$  to  $\mathbf{Q}_j$ , then the vector  $\mathbf{q}_{j+n}$  must be at the angle  $\pi - \alpha$  to  $\mathbf{Q}_j$ , so that  $\pi - 2\alpha = 2\pi n/N$  with integer  $n$ . At the same time, the value of  $\alpha$  should be as close as possible to  $\pi/6$ . Then  $\alpha/\pi = 1/2 - n/N$ , which leads to  $n \approx N/3$ . Any odd integer may be presented as  $N = 3m \pm 1$ , or  $N = 3m$  with integer  $m$ . Then the required value is  $n = m$ , and we find  $\alpha = \pi[1/2 - m/(3m \pm 1)]$  for  $N = 3m \pm 1$ , and  $\alpha = \pi/6$  exactly for  $N = 3m$ . For  $N = 11$ ,  $n = m = 4$ , one can choose the negative sign, arriving at  $\alpha = 3\pi/22$ . The required value can be achieved by reducing the wave number of the wave mode from  $q$  to  $q(1 - \epsilon_N)$ , where  $\epsilon_N \ll 1$  depends on  $N$ . The calculation for  $N = 11$  gives  $\epsilon_{11} \approx 0.048$ .

A strained resonant pattern has a simpler structure than the exact resonant planform because it is built up of only  $4N$  plane waves, and contains only two independent amplitudes:

$$\chi_1 = \sum_{j=1}^N [a_j e^{i\mathbf{Q}_j \cdot \mathbf{r}} + b_j e^{i\omega t} e^{i\mathbf{q}_j \cdot \mathbf{r}}] + \text{c.c.}, \quad (37)$$

where the amplitudes satisfy the following relations:

$$a_{j+1} = a_j, \quad b_{j+1} = -e^{i\Delta/2} b_j. \quad (38)$$

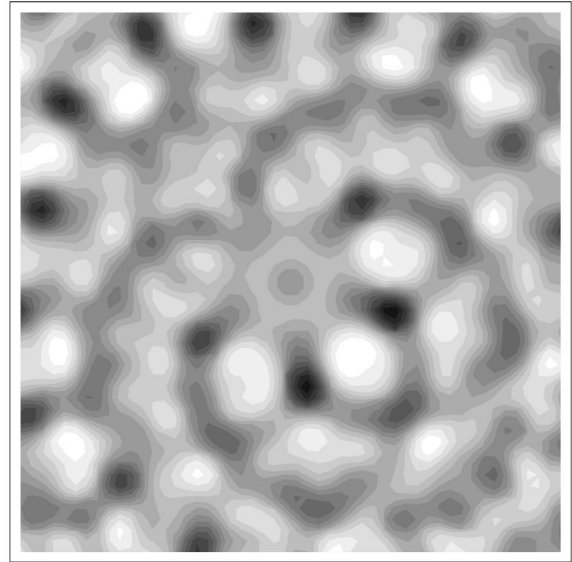
A snapshot of the planform defined by Eq. (37) and the corresponding structure in the Fourier space are shown in Fig. 3.

At first sight, the amplitude equations appear to be more involved in this case, since each elementary wave mode  $\mathbf{q}_j$  takes part in two resonant triangles:  $\mathbf{Q}_j = \mathbf{q}_j - \mathbf{q}_{j+n}$  and  $\mathbf{Q}_{N+j-n} = \mathbf{q}_{N+j-n} - \mathbf{q}_j$ . In order to derive the dynamic equations for the amplitudes  $a_j$  and  $b_j$  in the planform (37), we have to repeat the procedure used in the preceding subsection. This yields the following result:

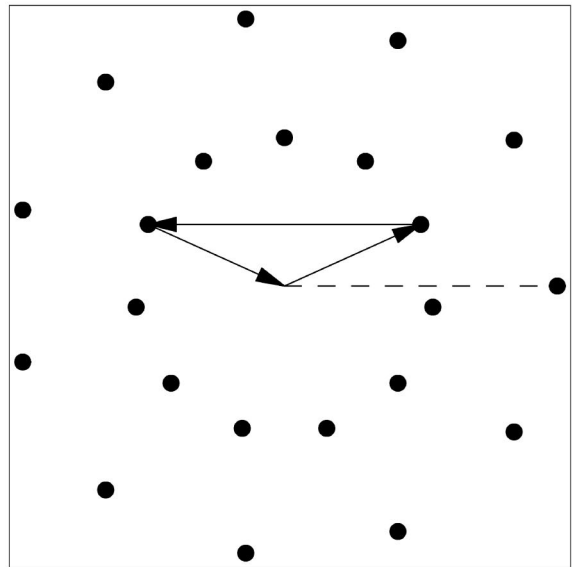
$$\begin{aligned} \dot{a}_j &= -2\kappa I_0 \sin^2(Q^2/2) b_j b_{j+n}^* - 2\kappa I_s \sin Q^2 a_{j-1}, \\ \dot{b}_j &= -2\kappa I_0 \sin^2(q^2/2) (a_j b_{j+n-1} + a_j^* b_{N+j-n-1}) \\ &\quad - 2\kappa I_w \sin q^2 b_{j-1}. \end{aligned} \quad (39)$$

Recalling the relations (38) we rewrite the above system as

$$\begin{aligned} \dot{a}_j &= -2\kappa I_s \sin Q^2 a_j + 2(-1)^{n+1} \kappa I_0 \sin^2(Q^2/2) \\ &\quad \times e^{-in\Delta/2} b_j b_j^*, \end{aligned}$$



(a)



(b)

FIG. 3. Strained resonant pattern defined by Eq. (37) with  $N = 11$ . (a) The real space image. The values or the amplitudes correspond to the stationary solution at  $\mu = -1/4$ . (b) The Fourier space structure. Explanations are as in Fig. 2.

$$\begin{aligned} \dot{b}_j &= 2\kappa I_w \sin q^2 e^{-i\Delta/2} b_j - 2\kappa I_0 \sin^2(q^2/2) \\ &\quad \times b_j [a_j (-e^{i\Delta/2})^{n-1} + a_j^* (-e^{i\Delta/2})^{N-n-1}]. \end{aligned} \quad (40)$$

Taking into account that  $(-e^{i\Delta/2})^N = 1$ , and denoting  $A = a_j e^{in\Delta/2}$  and  $B = b_j$ , we arrive at the following simple dynamical system:

$$\begin{aligned} \dot{A} &= \mu_s A + \nu_s |B|^2, \\ \dot{B} &= \mu_w e^{-i\Delta/2} B + \nu_w e^{-i\Delta/2} B (A + A^*), \end{aligned} \quad (41)$$

where

$$\begin{aligned} \nu_s &= (-1)^{n+1} 2\kappa I_0 \sin^2(Q^2/2), \\ \nu_w &= (-1)^n 2\kappa I_0 \sin^2(q^2/2), \end{aligned}$$

$$\mu_s = -2\kappa I_{1s} \sin Q^2, \quad \mu_w = 2\kappa I_{1w} \sin q^2. \quad (42)$$

#### D. Double resonance

The interactions of composite waves are more complicated when  $N$  is divisible by 3. In this case, one has to include also additional resonant terms corresponding to interaction of Turing modes comprising the Turing composite mode. The resonant conditions for these modes have the form  $\mathbf{Q}_j + \mathbf{Q}_{j+m} + \mathbf{Q}_{j+2m} = \mathbf{0}$ , where  $m = N/3$ . It must be noted that the resonance involving one Turing and two wave modes becomes in this case exact, i.e., it is excited at the values of wave numbers corresponding to the minima of the neutral curve.

Repeating the derivation procedure and recalling that  $Q^2 = 3\pi/2$  and  $q^2 = \pi/2$ , we arrive at the set of equations

$$\begin{aligned} \dot{a}_j &= 2\kappa I_{1s} a_j - \kappa I_0 [(-1)^m e^{-im\Delta/2} b_j b_j^* + a_j^{2*}], \\ \dot{b}_j &= -2\kappa I_{1w} e^{-i\Delta/2} b_j - \kappa I_0 b_j [a_j (-e^{i\Delta/2})^{m-1} \\ &\quad + a_j^* (-e^{i\Delta/2})^{N-m-1}]. \end{aligned} \quad (43)$$

Taking into account that  $(-e^{i\Delta/2})^N = 1$ , denoting  $A = a_j e^{im\Delta/2}$  and  $B = b_j$ , and rescaling the time variable by  $\kappa I_0$  yields a simple dynamical system:

$$\begin{aligned} \dot{A} &= 2\mu_s A + (|B|^2 + A^{2*}), \\ \dot{B} &= B e^{-i\Delta/2} [2\mu_w - (A + A^*)], \end{aligned} \quad (44)$$

where  $\mu_s = I_{1s}/I_0$ ,  $\mu_w = I_{1w}/I_0$ .

### V. AMPLITUDE DYNAMICS

#### A. Dynamics of three composite modes

The amplitude equations involving three composite modes have most interesting dynamics. It is advantageous to use the polar representation of the complex amplitudes,

$$a_j = \rho_a e^{i\theta_a}, \quad b_j = \rho_b e^{i\theta_b}, \quad c_j = \rho_c e^{i\theta_c}. \quad (45)$$

Then Eqs. (36) are reduced to the following system of four real equations including a single phase combination  $\theta = \theta_a + \theta_c - \theta_b$ :

$$\begin{aligned} \dot{\rho}_a &= \mu_s \rho_a - \nu \rho_b \rho_c \cos \theta, \\ \dot{\rho}_b &= \mu_w \rho_b \cos(\Delta/2) + \nu \rho_a \rho_c \cos(\theta - \Delta/2), \\ \dot{\rho}_c &= \mu_w \rho_c \cos(\Delta/2) + \nu \rho_a \rho_b \cos(\theta + \Delta/2), \\ \dot{\theta} &= \nu \left( \frac{\rho_b \rho_c}{\rho_a} \sin \theta - \frac{\rho_a \rho_b}{\rho_c} \sin(\theta + \Delta/2) - \frac{\rho_a \rho_c}{\rho_b} \sin(\theta - \Delta/2) \right). \end{aligned} \quad (46)$$

The stationary values of the amplitudes  $\rho_a, \rho_b, \rho_c$  can be expressed as

$$\rho_a = \frac{\mu_w \cos(\Delta/2)}{\nu \sqrt{\cos(\theta - \Delta/2) \cos(\theta + \Delta/2)}}, \quad (47)$$

$$\rho_b = \frac{1}{\nu} \sqrt{\frac{-\mu_s \mu_w \cos(\Delta/2)}{\cos(\theta + \Delta/2) \cos \theta}},$$

$$\rho_c = \frac{1}{\nu} \sqrt{\frac{-\mu_s \mu_w \cos(\Delta/2)}{\cos(\theta - \Delta/2) \cos \theta}}.$$

The stationary value of the phase  $\theta$  verifies the following equation:

$$\mu_s \left( \tan \theta + \mu \frac{\sin 2\theta}{\cos(\theta - \Delta/2) \cos(\theta + \Delta/2)} \right) = 0, \quad (48)$$

where  $\mu = \mu_w \cos(\Delta/2) / \mu_s$ . A simple solution of this equation satisfies  $\sin \theta = 0$ , yielding  $\theta = \pi$  at negative  $\mu_s$ , and  $\theta = 0$  for positive value of  $\mu_s$ . This is a symmetric solution with equal amplitudes of the wave modes:  $\rho_b = \rho_c = \sqrt{-\mu_s \mu_w / \nu}$ . Applying the Routh-Hurwitz stability criterion one can check that the stability conditions of the symmetric solution are

$$\mu_w > 0, \quad \mu > -1/4, \quad \mu_s < -\frac{1}{2} \cos^2(\Delta/2). \quad (49)$$

Another solution of Eq. (48) verifies the relation

$$\cos^2 \theta = \frac{\sin^2(\Delta/2)}{1 + 2\mu}. \quad (50)$$

It is immediately seen that the solution exists provided  $\mu > -1/2$  and  $1 + 2\mu \geq \sin^2(\Delta/2)$ , which leads to the condition  $\mu \geq -\frac{1}{2} \cos^2(\Delta/2)$ . It is required for positiveness of the amplitudes that  $\cos(\theta - \Delta/2) \cos(\theta + \Delta/2) > 0$ . This inequality can be rewritten in the form  $\mu \sin^2(\Delta/2) < 0$ , and hence,  $\mu < 0$ . Equation (50) defines in fact a pair of asymmetric solutions which are transformed to one another by interchanging the amplitudes of the wave modes. This pair bifurcates from the symmetric solution at  $\mu = -\frac{1}{2} \cos^2(\Delta/2)$ . The bifurcation is supercritical at  $\mu > -\frac{1}{4}$ .

At still higher values of  $\mu$ , the asymmetric solutions undergo a supercritical Hopf bifurcation. The bifurcation locus in the plane  $(\Delta, \mu)$  is given implicitly by the relation

$$\begin{aligned} &-(1 + 4\mu)(1 + 5\mu + 8\mu^2) \sin^4(\Delta/2) \\ &+ [3 + 8\mu(\mu + 2)(1 + 2\mu)] \sin^2(\Delta/2) [2\mu + \cos^2(\Delta/2)] \\ &+ 3(4 + 7\mu + 4\mu^2) [2\mu + \cos^2(\Delta/2)]^2 = 0. \end{aligned}$$

The additional stability condition is  $\mu_s < 0$ .

A pair of asymmetric periodic solutions further merges into a symmetric attractor as a result of a homoclinic bifurcation. We were unable to determine the locus of this bifurcation exactly because of a very complicated dynamics in the vicinity of a saddle point in the four-dimensional phase space. This is a saddle focus with two-dimensional stable and unstable manifolds, both oscillatory. Near this boundary, the dynamics is apt to be chaotic [18]. The behavior of the periodic orbit rather close to the saddle-loop bifurcation is seen in Fig. 4. Near the saddle point, one of the amplitudes becomes nearly extinct, while the composite phase undergoes sharp oscillations. Our numerical estimates suggest that

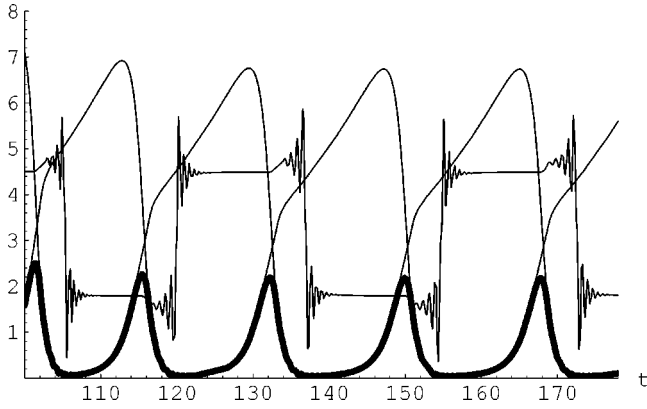


FIG. 4. Periodic solution of the system Eq. (46) for  $N=11$  at  $\mu_w/\mu_s = -1/20$ . The composite phase  $\theta$  remains nearly constant during a larger part of each half period, and undergoes sharp oscillations before and after switching to the alternative level. Oscillations of the two wave modes are identical but shifted by the half period relative to one another. Oscillations of the Turing mode (thick line) have a smaller amplitude, and a twice shorter period.

the saddle-loop boundary is roughly defined by the relation  $\mu = -\pi\Delta/2$ . At  $\mu < -\frac{1}{4}$ , the system escapes to infinity, while at  $\mu > 0$ , i.e.,  $\mu_s < 0$  and  $\mu_w < 0$ , the pattern decays to the trivial featureless state. The bifurcation diagram in the plane  $\mu, \Delta$  is presented in Fig. 5.

The actual pattern may be stabilized at large amplitudes by nonresonant cubic interactions. Confinement in the small-amplitude region by quadratic interactions is only possible when the Turing mode is subcritical and the wave mode is supercritical but not too strongly. At  $N=11$ , the small-amplitude dynamics never relaxes to a stationary state. Long-time oscillations of the type shown in Fig. 4 modulate the nonstationary quasicrystalline structure shown in Fig. 2.

### B. Dynamics of two composite modes

The dynamic behavior under conditions of strained resonance is much simpler. One can see that the relevant dynamic variables in Eqs. (41) are the real part of the compos-

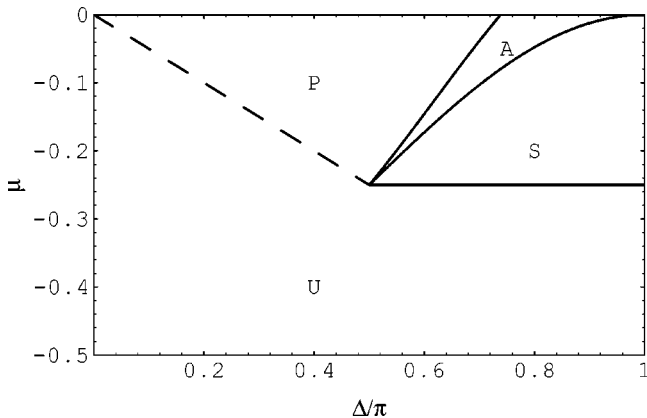


FIG. 5. Bifurcation diagram of Eq. (46) in the parametric plane  $(\Delta, \mu)$ . Letters  $S$  and  $A$  denote the regions of stable stationary symmetric and asymmetric solutions;  $P$  stands for a pair of asymmetric periodic solutions, and  $U$  for a symmetric periodic solution or other symmetric dynamic attractor. The dashed line shows an approximate location of the saddle-loop bifurcation.

ite Turing mode  $R = \text{Re } A$  and the modulus of the wave mode  $P = |B|^2$ . Transforming to these variables we obtain the system of two real equations only:

$$\dot{R} = \mu_s R + \nu_s P, \quad \dot{P} = 2P(\mu_w + 2\nu_w R)\cos(\Delta/2). \quad (51)$$

The stationary solution is

$$R = -\frac{\mu_w}{2\nu_w}, \quad P = \frac{\mu_w \mu_s}{2\nu_w \nu_s}. \quad (52)$$

According to Eq. (42),  $\nu_w \nu_s < 0$ , and the above solution exists only if  $\mu_w \mu_s < 0$ . The stability conditions of the solution are  $\mu_s < 0$ ,  $\mu_w > 0$ , and  $\cos(\Delta/2) > 0$ . Thus the stability region is greatly enlarged, compared to the exact resonance, and encompasses now the entire quadrant  $\mu < 0, 0 < \Delta < \pi$  in Fig. 5, while periodic long-time dynamics is not seen anymore.

### C. Double resonance dynamics

Equations (44) including double resonance differ from Eq. (41) only by the presence of a self-interaction term for the Turing composite mode. This term is destabilizing, and, in the case of pure Turing patterns, one needs to include third-order terms dependent on four-wave interactions to ensure amplitude saturation. We shall see that, due to the quadratic wave-Turing resonance, the pattern can be stabilized in the small-amplitude region. The system, however, still possesses a large-amplitude attractor.

Setting in Eq. (44)  $A = re^{i\theta}$ ,  $B = pe^{i\tau}$  yields

$$\dot{r} = 2\mu_s r + (p^2 \cos\theta + r^2 \cos 3\theta),$$

$$\dot{p} = 2p(\mu_w - r \cos\theta)\cos(\Delta/2),$$

$$\dot{\theta} = -(p^2 \sin\theta + r^2 \sin 3\theta)/r. \quad (53)$$

The phase of the wave mode is irrelevant also in this case, so that the equation for  $\tau$  is separated and may be dropped. The phase of the Turing mode relaxes to zero; thus the stationary solution is

$$\theta = 0, \quad r = \mu_w, \quad p = -\mu_s \sqrt{-\mu(\mu+2)}, \quad (54)$$

where  $\mu = \mu_w/\mu_s$ . The solution exists at  $\mu_w > 0$ ,  $\mu_s < 0$ ,  $0 > \mu > -2$ . For stability analysis, it is sufficient to consider a simplified system with  $\theta=0$ :

$$\dot{r} = 2\mu_s r + p^2 + r^2,$$

$$\dot{p} = 2p(\mu_w - r)\cos(\Delta/2). \quad (55)$$

The trace of the linearized system is  $2(\mu_s + \mu_w)$ ; thus a Hopf bifurcation takes place at  $\mu = -1$ . This bifurcation is subcritical. The stationary state is stable at  $0 > \mu > -1$  but the system always possesses an additional attractor

$p \rightarrow 0, r \rightarrow \infty$ . An unstable orbit which exists at  $\mu > -1$  bounds the attraction domain of the small-amplitude stationary solution. At  $\mu < -1$ , all trajectories are attracted to the large-amplitude region, and taking into account higher-order terms is necessary to obtain finite solutions.

## VI. CONCLUSION

The nonlinear optical cavity with a rotated beam has a versatile and easily controllable dynamics. Complex small-amplitude patterns near a symmetry-breaking bifurcation

point, that are very difficult to construct in other pattern-forming nonequilibrium systems, appear here in a very natural way. The central point of this study is a primary role of resonant interactions between wave and Turing modes.

## ACKNOWLEDGMENTS

This research has been supported in part by the EU TMR network "Nonlinear dynamics and statistical physics of spatially extended systems." L.M.P. acknowledges the support by the Fund for Promotion of Research at the Technion.

- 
- [1] S. A. Akhmanov, M. A. Vorontsov, V. Yu. Ivanov, A. V. Larichev, and N. I. Zheleznykh, *J. Opt. Soc. Am. B* **9**, 78 (1992).
  - [2] E. Pampaloni, S. Residori, and F. T. Arecchi, *Europhys. Lett.* **24**, 647 (1993).
  - [3] E. Pampaloni, P. L. Ramazza, S. Residori, and F. T. Arecchi, *Phys. Rev. Lett.* **74**, 258 (1995).
  - [4] S. Residori, P. L. Ramazza, E. Pampaloni, S. Boccaletti, and F. T. Arecchi, *Phys. Rev. Lett.* **76**, 1063 (1996).
  - [5] E. Pampaloni, S. Residori, S. Soria, and F. T. Arecchi, *Phys. Rev. Lett.* **78**, 1042 (1997).
  - [6] H. Adachihara and H. Faid, *J. Opt. Soc. Am. B* **10**, 1242 (1993).
  - [7] L. M. Pismen, *Phys. Rev. A* **23**, 334 (1981).
  - [8] L. M. Pismen, *Dynamics Stability Syst.* **1**, 97 (1986).
  - [9] B. A. Malomed, A. A. Nepomnyashchy, and M. I. Tribelsky, *Phys. Rev. A* **42**, 7244 (1991).
  - [10] B. Christiansen, P. Alstrom, and M. T. Levinsen, *Phys. Rev. Lett.* **68**, 2157 (1992).
  - [11] W. S. Edwards and S. Fauve, *Phys. Rev. E* **47**, R788 (1993).
  - [12] H. W. Müller, *Phys. Rev. A* **49**, 1273 (1994).
  - [13] A. A. Golovin, A. A. Nepomnyashchy, and L. M. Pismen, *Physica D* **81**, 117 (1995).
  - [14] D. Leduc, M. Le Berre, E. Ressayre, and A. Tallet, *Phys. Rev. A* **53**, 1072 (1996).
  - [15] M. Le Berre, D. Leduc, E. Ressayre, and A. Tallet, *Phys. Rev. A* **54**, 3428 (1996).
  - [16] M. Le Berre, S. Patrascu, E. Ressayre, A. Tallet, and N. I. Zheleznykh, *Chaos Solitons Fractals* **4**, 1389 (1994).
  - [17] Yu. A. Logvin, B. A. Samson, A. A. Afanas'ev, A. M. Samson, and N. A. Loiko, *Phys. Rev. E* **54**, R4548 (1996).
  - [18] P. Colinet, Ph. Géoris, J. C. Legros, and G. Lebon, *Phys. Rev. E* **54**, 514 (1996).
  - [19] L. M. Pismen, *J. Colloid Interface Sci.* **102**, 237 (1984).
  - [20] M. R. E. Proctor and C. A. Jones, *J. Fluid Mech.* **188**, 301 (1988).
  - [21] A. C. Newell and J. V. Moloney, *Nonlinear Optics* (Addison-Wesley, Reading, MA, 1992).
  - [22] G. D'Alessandro and W. R. Firth, *Phys. Rev. Lett.* **66**, 2597 (1991).